

Employing the Cascode Methods, A Transformer-Less High Voltage Gain Step-Up DC-DC Converter

Basim Khalid Mohammed Ali ^{1, *}, , Wisam Hasan Ali ^{2,3},  and Noor Hameed Jalil ⁴, 

¹ Peter the Great St. Petersburg Polytechnic University (SPbPU), Saint Petersburg, Russia; basim.KM@spbpu.edu.ru

² School of Electrical and Electronic Engineering, Engineering campus, Universiti Sains Malaysia (USM), Penang, Malaysia; wisam@student.usm.my

³ Electronic and Communication Engineering, Çankaya University, Ankara, Turkey

⁴ Department of Computer Engineering Information Technology, Çankaya University, Ankara, Turkey; noor-@ceit.cankaya.edu.tr

* Correspondence; Tel.: +7-9312449642

Abstract: The goal of this research is to use the cascode approach to buck boost converters in order to produce high step-up voltage gain with a suitable duty ratio for an electric energy conversion system. Electronic equipment that demand electricity must convert AC voltage sources into DC power since they cannot be powered directly by the current electrical AC voltage. Significant voltage increases cannot be achieved by traditional boost converters because of the influence of power switches, parasitic resistive parts, and the diodes' reverse-recovery issue. The high voltage gains step-up (HVGSU) DC-DC converter, which combines two integrated buck-boost converters with a single switch, is proposed in this study. With the cascode technique, high voltage gain can be obtained without an extreme duty ratio; in this case, the switch's duty ratio is regulated by PWM technology. There is a thorough discussion of the suggested converter's equipment and modeling.

Keywords: Amplifier converter; cascode method; dc to dc converter; high voltage gain step-up

1. Introduction

Worldwide, alternative power supplies are favored because they provide a clean, pollution-free, and environmentally friendly atmosphere [1-3]. Electric cars powered by renewable energy sources (RESs) will be crucial for transportation in the future. High step-up voltage gain is typically the result of lower voltage achieved from photovoltaic cells. To achieve the required voltage levels, DC-DC converters are advised [4]. For instance, high-intensity discharge lights used in automotive applications require a higher working voltage than the battery voltage [5]. Applications for HVGSU DC-DC Converters include UPS, conversion of energy from renewable sources, and industry testing [6]. A high ac input voltage is additionally necessary in boost PFC circuits to achieve low THD and high-power factor [7, 8].

Generally speaking, reverse recovery issues with the diodes and parasitic components make smooth high voltage gain impossible. Fly back converters can enable HVGSU, but the transformer's leakage capacitance restricts the voltage stress on the switches [9-11]. Efficiency is increased by the HSUVG in addition to voltage levels. Numerous approaches are used in the literature to achieve HV with fewer switches and increase economy; these are explained as follows: In order to improve the conversion rate and lessen the voltage stress on the switches, a novel DC-DC converter topology is presented [10, 12, 13]. A single-switch DC to DC converter is suggested, which lowers the loss of switching and issues with reverse recovery [14]. It is suggested to use the cascode approach in

Citation: To be added by editorial staff during production.

Academic Editor: Dr. Oladimeji Ibrahim

Received: 27/5/2024

Revised: 2/6/2024

Accepted: 8/6/2024

Published: 14/6/2024



Copyright: © 2024 by the authors. Submitted for possible open access publication under the terms and conditions of the Creative Commons Attribution (CC BY) license (<https://creativecommons.org/licenses/by/4.0/>).

conjunction with a transformer-less DC-DC converter to lessen the voltage and current pressures on the switches [10, 15]. It is suggested to use a voltage multiplier with an inter-laced conversion for power control uses, like electric cars [1]. To obtain high voltage, a DC-DC converter with a connected inductor is suggested [5]. For superior converting energy with greater power factor, a soft switching technique is suggested in conjunction with a PWM and PFC controller [16]. Transformers, linked inductors, and switching capacitors are avoided with a bidirectional H-bridge DC-DC converter with DC link [2]. When using a bidirectional DC-DC converter that is constructed using SVM technique instead of a traditional DC-DC converter with PWM technique, large capacitor stacks can be removed. For HVDC applications, a DC-DC converter with MPPT is suggested for converting a 10–40v PV cell to 300v [17]. To increase the effectiveness of conversion, a low-cost single-ended converter with isolation and non-isolation configuration is suggested [4].

This study suggests an HVGSU DC-DC converter that uses PWM technology instead of a transformer. This setup works quite well with RESs that have links to the network [18-20].

2. Materials and Methods

2.1 High- Voltage Output Amplifier Converter for Cascade

A transformer-less high step-up DC to DC converter using the cascode method is proposed in this paper. Figure 1 shows the suggested converter's circuit layout

Table 2: Voltage Gain of traditional and Cascode Converter for Diverse Load Rate

Load Cycle	Conventional amp. Converter	Cascode amp. Converter
0.1	1.09	0.19
0.2	1.19	0.48
0.3	1.39	0.98
0.4	1.71	1.69
0.5	1.98	2.99
0.6	2.47	4.98
0.7	3.27	9.09
0.8	4.84	23.98
0.9	9.76	98.96

Table 1: Imaginary designs of High-Voltage Increase step up DC-DC Converter

Vi (V)	Ii (A)	Pi (W)	V0 (V)	Io (A)	Po (W)	RL(Ω)	η%
24	1.19	30	200	0.2	21	2020	68
23.9	2.48	62	200	0.3	41	1030	66
24	3.48	85	200	0.4	61	670	71
23.9	4.58	112	200	0.5	81	550	72
24	5.76	138	200	0.6	99	460	73

Table 1 describes the theoretical results under different load circumstances. Under full load, the conversion efficiency is 73.9%. 99.9 watts is the output power and 136.99 watts is the source of power under full load circumstances.

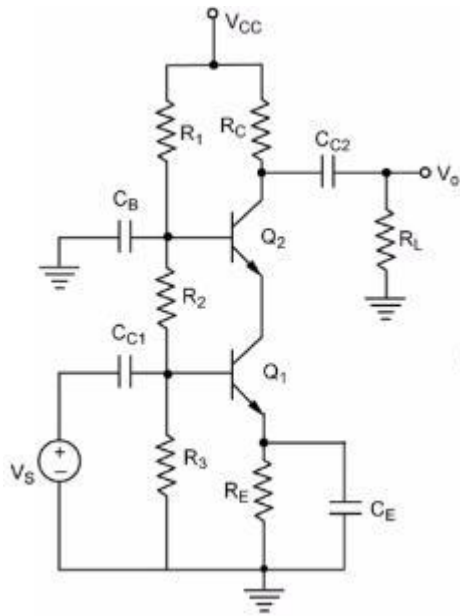


Figure 1. Circuit diagram of the planned cascode converter

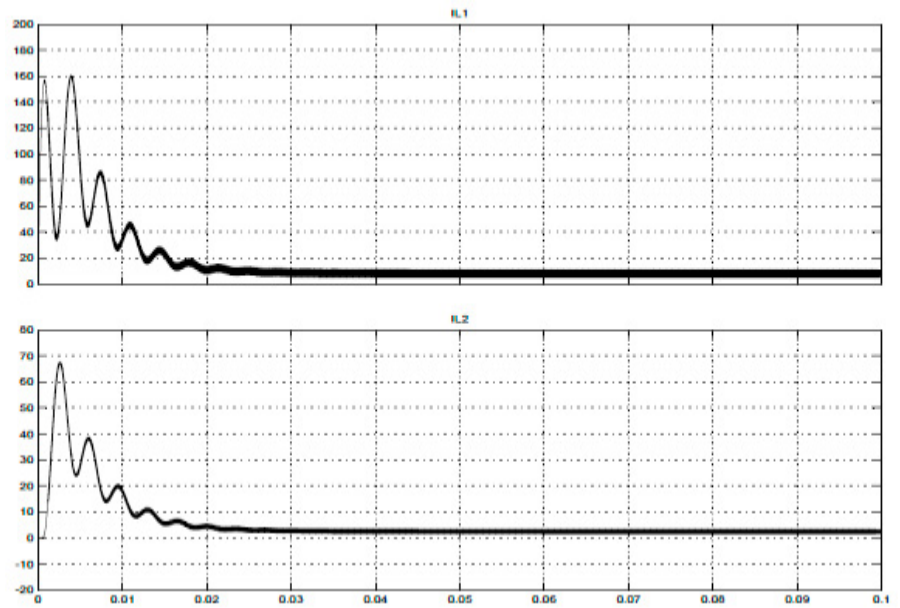


Figure 2. Inductor transient streams for open loop cascode converter

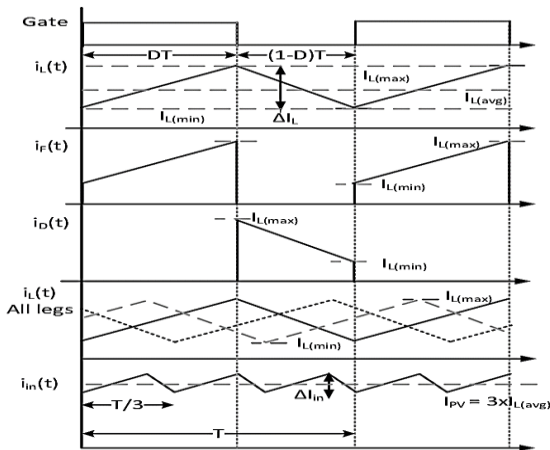


Figure 3. Diode currents of a closed loop cascode converter

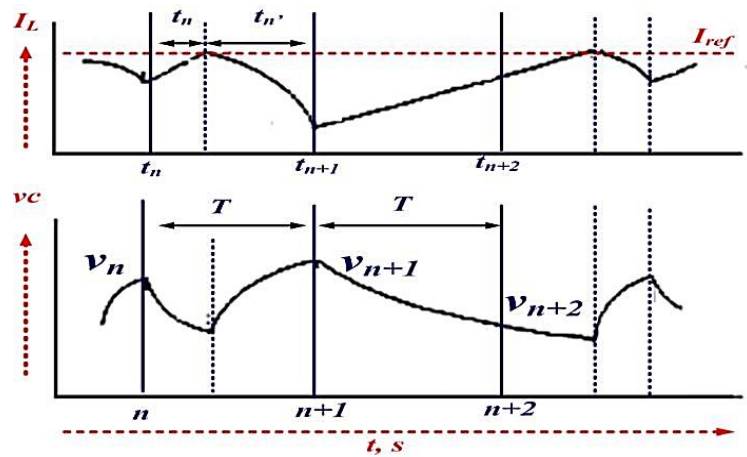


Figure 4. Inductor currents of a closed loop cascode converter

2.2 Strict Cascode Amplifier Converter Design

The suggested converter's operational structure is shown in Figure 4. There are two phases in this block illustration: the power phase and the control phase. The power phase comprises a high voltage gain boost converter built on the cascode technology and a DC input supply that ranges from 23.9 to 39.9 volts. 200 volts DC, the power phase's results, is fed back into the voltage feedback. The image connector, pulse width modulation controller, and voltage feedback make up the control phase. Here, TL493 IC is utilized as a pulse width modulated controller, TLP249 IC is used as a photo coupler, and CA3139 IC is used as voltage feedback.

A high voltage gains improvement converter based on the cascode method receives an input voltage of 23.9 volts. Its output, 199 volts, is sent to voltage feedback, and the resistor combo is used to lower the 199 volts to 4.99 volts. The CA3139 compensation, which serves as a feedback IC, receives this 4.99V. The +4.99V reference is then sent to the IC TL493 pulse generator, which produces a pulse with a magnitude of +4.99V, but not

enough to activate the MOSFET switch. In addition to serving as an isolation device, the TLP249 photo coupler is utilized to boost the pulse's magnitude from +4.99 Volts to, say, +14.99 Volts. The IRFP459 MOSFET receives a pulse with a magnitude of +14.99 V. The cascode converter circuit schematic for hardware execution is shown in Figure 4. The input capacitance (I_{ds}), which is linked across the MOSFET, is drained in this system by the MOSFET operating as a switch. Table 3 provides the cascode converter's characteristics.

3. Results

3.1 Discussion

Equations (1) and (2) provide the final benefits of the standard and cascode converters as a result of work rate.

$$\frac{V_o}{V_i} = \frac{1}{v} \quad (1)$$

$$\frac{V_o}{V_i} = \frac{2D-D^2}{v} \quad (2)$$

Table 2 makes it evident that if the load ration is greater than 0.41, the voltage win of the suggested converter is greater than the voltage increases of the amplifier converter. Therefore, by taking into account an efficiency period higher than 0.389, a cascode arrangement can yield a significant step-up voltage increase. The cascode converter with both open and closed loop execution, as well as the traditional boost conversion, are all simulated. Table 3 provides the suggested converter's characteristics.

Table 3. Specifications of the Cascode converter

Restriction	Value
V_{in}	24 V
V_o	199V
P_o	99 W
f_{os}	49 kHz
Co_1	679 μ F
Co_2	679 μ F
L_1	52.5 μ H
L_2	64 μ H
K_p	0.0002
K_i	0.099

Table 4. Evaluation of inductor passing currents

Open Loop Current	Closed Loop Current
Peak Amplitude: 161 Amps	23 Amps
Transient Period: 0.3 S	0.099 sec
Settling Period: 0.2 S	0.059 sec

The waveform shapes of a typical amplifier converter are shown in Figures 2. It shows the gate's signal of an amplifier converter and shows the input the voltage, results voltage, current, and current of an amplifier converter. Figure 3 display the diode currents, inductor currents, input voltage, current, output voltage, current, and inductor transient currents of an open- and closed loop cascode converter.

The task is to take a specific input energy of 23.9V and turn it into a final voltage of 200V. The voltage that came out of the closed-loop cascode converter quickly surpassed that of each of the dual converters, reaching 49.9V. (See Figures 2 and 3) This is acquired from the DC supply and the rear semi stage input. On the other hand, the output voltages of the two semi-stages added together via cascade form the ultimate output voltage of the suggested converter. Figures 2 and 3 show an analysis of the inductor electrical currents for cascode converters with open and closed loops. While the inductor currents in an open loop cascode converter settle more slowly, the highest intensity of 159.81 A is significantly higher than that of a closed cascode converter, which is approximately 22.8 A. Table 4 provides a comparison of standard, open loop, and closed cascode converters.

3.2 Trial Findings

The control phase and power phase comprise both sections of the work's hardware execution. These are described in brief in the parts that proceed.

3.2.1 Control Phase

The TL493 (PWM Generator), TLP249 (Isolator), CA3139 (Compensator), and 7813 & 7814 Governors were the parts utilized in the control phase. As illustrated in Figure 5, the cutting teeth waveform and reference voltages are compared to produce the gate pulses for a MOSFET using the pulse width modulation (PWM) approach. The 4.9-volt gate pulse produced by the TL493 PWM Inverter in this instance (Figure 6) is insufficient to turn on an IRFP459 MOSFET. Therefore, the 4.9-volt gate pulsing is multiplied to the 14.9-volt pulse seen in Figure 6 using a TLP249 optical isolator. It functions as an absorber as well. When the TL493 is coupled to the electrical circuit, it generates impulses in the system with a frequency for switching of 49.9 KHz and load rates of 0.959, 0.679, 0.249, and 0.899, accordingly, as shown in Figure 6.

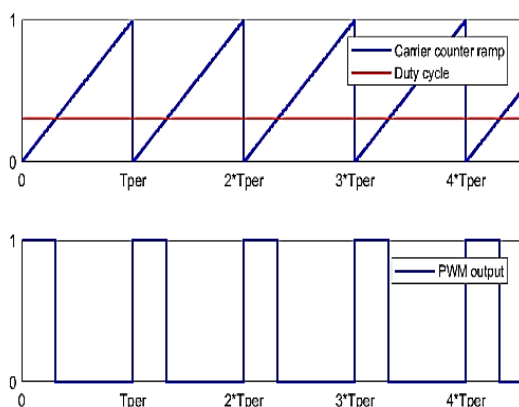


Figure 5. PWM Comparison (V_{ref} & $V_{carrier}$)

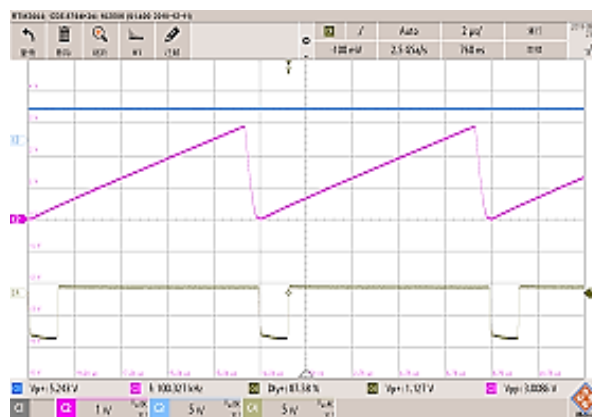


Figure 6. Gate Pulse from TL493 with Load rate

3.2.2 Phase of Energy

The IRFP459 MOSFET, two inductors, two capacitors, and four diodes are the parts of the electrical power phase that are seen in Figure 7. The resulting voltage, which is a constant DC value of 199 volts, is displayed in Figure 8. The current that is output for $RL=679.9$ Ohms, or continuous DC current, is shown in Figure 8, and the input current and gate pulses are delivered to MOSFET IRFP459 in Figure 9. Inductor Current (IL1) and Inductor Current (IL2) are shown in Figures 9, respectively. Inductor L1 current (IL1) is also found to be greater than inductor L2 current (IL2).

A contrast of the simulated and experimental data is presented in Table 5. Table 6 shows that in both modeling and experiments, the resultant voltage produced is 199 volts for an identical starting voltage of 23.9 volts. In the modeling and experimentation, the resultant effectiveness is 69.96% and 69.12%, correspondingly. There is substantial agreement regarding the outcomes of the model and the results of the experiment. Tables 6 and 7 provide the design specifications and the electric layout for the suggested converter, accordingly.

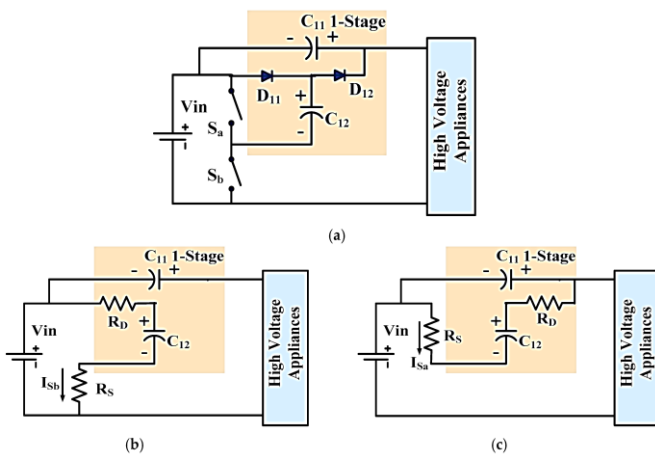


Figure 7. Mechanisms employed in energy phase of a planned converter in hardware execution

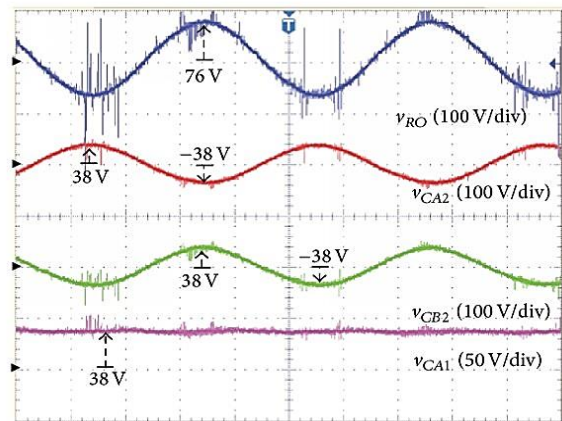


Figure 8. Production voltage from the cascode converter

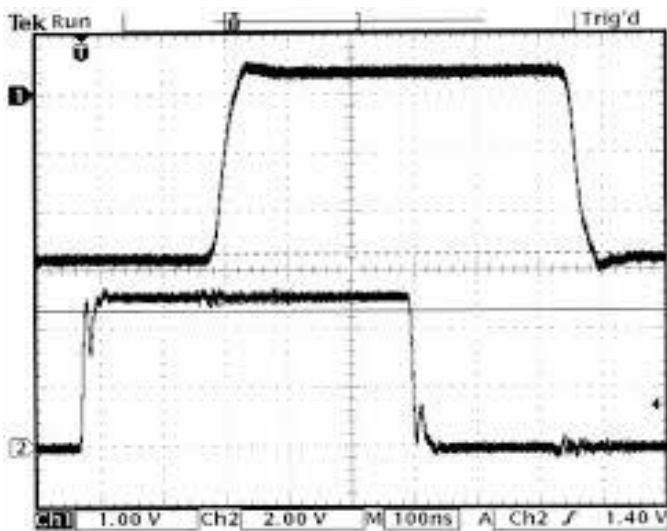


Figure 9. Input production & Gate Pulse specified to the MOSFET

Table 5. Contrast of Replication and Hardware outcomes

Restrictions	Closed Loop Cascode amp. Converter	
	Since Imitation	Since Trial
V_i (V)	23.9	23.9
R_L (Ω)	679	679
I_i (A)	3.39	3.49
D	0.669	0.679
PI (W)	82.39	83
V_O (V)	199	199
I_O (A)	0.291	0.29
PO (W)	58.19	57
η (%)	70.59	69.39

Table 6. Proposal Obligation

V_{in}	24 – 39.9 v
V_{Out}	199 V
I_{Out}	0.49 A
Fsw	49.1 kHz
Pout	99.8 W

Table 7. Proposal Scheming

L1	52 μ H / 9 A
L2	635 μ H / 4A
C1 and C2	679 μ F / 449 v
D1 – D4	14.9 A
S1	29 A, 449 v

153

154

155

156

157

5. Conclusions

This study presents the hardware components and simulations of a high step-up DC-DC converter. The findings of the simulated circuit and the real-world circuit are observed to be quite similar. The architecture makes use of the cascode approach to get a suitable duty ratio along with a high voltage gain. A prototype in the lab is shown to confirm the results. The outcomes of the simulation and experiment are obtained and analyzed. Considering the switching loss of the cascoded buck-boost converter with different expenses, the switching loss will worsen at high switching frequencies. Reducing switching losses is necessary in order to increase effectiveness and frequently switching. The Zero-Voltage-Switching method is a useful way to tackle this issue. In this approach, the electrical power converter's frequency of switching can be significantly increased without lowering the converter's effectiveness.

Acknowledgments: "This project would not have been possible without the generous financial support of the Peter the Great St. Petersburg Polytechnic University (SPbPU), Saint Petersburg, Russia. Lastly, I would like to acknowledge the study participants who generously shared their time and insights".

Conflicts of Interest: Declare conflicts of interest or state "The authors declare no conflict of interest."

References

1. Tseng, K.-C., C.-T. Chen, and C.-A. Cheng, *A High-Efficiency High Step-Up Interleaved Converter with a Voltage Multiplier for Electric Vehicle Power Management Applications*. Journal of Power Electronics, 2016. **16**: p. 414-424. 178-180
2. Zhang, Y., et al., *High Ratio Bidirectional DC-DC Converter with a Synchronous Rectification H-Bridge for Hybrid Energy Sources Electric Vehicles*. Journal of power electronics, 2016. **16**: p. 2035-2044. 181-182
3. Kadhim Abed, Q., L. Hikmet Mahdi, and A. Qays Abdullah, *Improved Command and Control (C2) capabilities in urban and challenging terrains*. Edison Journal for electrical and electronics engineering, 2023. **1**: p. 1-5. 183-184
4. Kim, D.-H., et al., *High Efficiency High-Step-up Single-ended DC-DC Converter with Small Output Voltage Ripple*. Journal of power electronics, 2015. **15**: p. 1468-1479. 185-186
5. Liu, H., J. Ai, and F. Li, *A Novel High Step-Up Converter with a Switched-Coupled-Inductor-Capacitor Structure for Sustainable Energy Systems*. Journal of Power Electronics, 2016. **16**: p. 436-446. 187-188
6. Moradzadeh, M., et al., *Novel High Step-Up DC/DC Converter Structure Using a Coupled Inductor with Minimal Voltage Stress on the Main Switch*. Journal of power electronics, 2016. **16**. 189-190
7. Liang, T.J., et al., *Novel Isolated High-Step-Up DC-DC Converter With Voltage Lift*. IEEE Transactions on Industrial Electronics, 2013. **60**(4): p. 1483-1491. 191-192
8. Mahmood Khudhur, A., F. Ghazi Saber, and M.A.K. Alsaedi, *Single-switch PWM converters for DC-to-DC power with reliability tolerance for battery power purposes*. Edison Journal for electrical and electronics engineering, 2024. **2**(1): p. 12-19. 193-194
9. Shen and Chen, *Dual-Input Isolated DC-DC Converter with Ultra-High Step-Up Ability Based on Sheppard Taylor circuit*. Electronics, 2019. **8**: p. 1125. 195-196
10. Kumari, N.K., D.S.G. Krishna, and M.P. Kumar, *Transformer Less High Voltage Gain Step-Up DC-DC Converter Using Cascode Technique*. Energy Procedia, 2017. **117**: p. 45-53. 197-198
11. Ahmed Kadhim, A., A. M. Al-Jumaili, and K. Hussain, *Converter for Voltage Source HVDC Links: Current Status and Future Challenges*. Edison Journal for electrical and electronics engineering, 2023. **1**: p. 17-23. 199-200
12. Shu, L.J., et al. *Transformerless high step-up DC-DC converter using cascode technique*. in *The 2010 International Power Electronics Conference - ECCE ASIA - 2010*. 201-202
13. Papanikolaou, N.P. and E.C. Tatakis, *Active voltage clamp in flyback converters operating in CCM mode under wide load variation*. IEEE Transactions on Industrial Electronics, 2004. **51**(3): p. 632-640. 203-204
14. Lin, B.R. and F.Y. Hsieh, *Soft-Switching Zeta-Flyback Converter With a Buck-Boost Type of Active Clamp*. IEEE Transactions on Industrial Electronics, 2007. **54**(5): p. 2813-2822. 205-206
15. Jaenul, A. and B.N.A. Altameemi, *Triple-Level Single-Ended Main Inductor Converter (SeMLC) with regard to Wind-Solar Hybrid Energies*. Edison Journal for electrical and electronics engineering, 2024. **2**(1): p. 20-26. 207-208
16. Esfandiari, G., H. Aran, and M. Ebrahimi, *Compherensive Design of a 100 kW/400 V High Performance AC-DC Converter*. Advances in Electrical and Electronic Engineering, 2015. **13**: p. 417-429. 209-210
17. Petit, P., et al., *New architecture for high efficiency DC-DC converter dedicated to photovoltaic conversion*. Energy Procedia, 2011. **6**: p. 688-694. 211-212
18. Tseng, K.C., C.C. Huang, and W.Y. Shih, *A High Step-Up Converter With a Voltage Multiplier Module for a Photovoltaic System*. IEEE Transactions on Power Electronics, 2013. **28**(6): p. 3047-3057. 213-214
19. Islam, M.R., et al., *Optimal Design of High-Frequency Magnetic Links for Power Converters Used in Grid-Connected Renewable Energy Systems*. IEEE Transactions on Magnetics, 2014. **50**(11): p. 1-4. 215-216
20. Bryant, B. and M.K. Kazimierczuk, *Voltage-Loop Power-Stage Transfer Functions With MOSFET Delay for Boost PWM Converter Operating in CCM*. IEEE Transactions on Industrial Electronics, 2007. **54**(1): p. 347-353. 217-218